Classical stabilization of periodically kicked hydrogen atoms

Giulio Casati, Italo Guarneri, and Giorgio Mantica
Università di Milano, sede di Como, via Lucini 3, 22100 Como, Italy
(Received 6 April 1994; revised manuscript received 29 June 1994)

We investigate the stability of a classical three-dimensional hydrogen atom subject to a periodic train of alternating δ-like pulses, or "kicks." The intense-field stabilization effect, widely investigated for the case of monochromatically driven atoms, is numerically shown to occur in this purely classical model, and its dependence on various parameters is analyzed. Our results support the view that classical intense-field stabilization is determined by the stability of the motion in a direction transverse to the field polarization, and confirm previously established estimates for the onset of stabilization.

PACS number(s): 31.50.+w, 32.80.Rm, 42.50.Hz

When a beam of hydrogen atoms prepared in some initial state interacts for a certain time with a radiation field of given intensity and frequency, some of the atoms are ionized, the ionization probability being a function of the initial state, the interaction time, and the field intensity and frequency as well. *Ceteris paribus,* one would naively expect this function to be monotonic in the field intensity, i.e., a stronger field should always produce a larger ionization. This expectation is contradicted by theoretical investigations that have shown that, on the contrary, on increasing the field strength above a critical value the hydrogen atom becomes increasingly stable against field-induced ionization. This surprising effect, known as intense-field stabilization (IFS), was originally predicted on purely quantal grounds [1], but has subsequently been found even in classical systems, first in simplified one-dimensional (1D) models using a smoothed Coulomb potential [4], and then in realistic 3D models [2,3]. A purely classical approach to IFS has yielded a rough theoretical estimate for the intensity border above which IFS should be expected [2]. Being thus clear that quantum IFS is paralleled by a quite similar classical phenomenon [5], the conclusion that the two phenomena have a common origin seems inescapable. Although only the quantum phenomenon is physically relevant in the atomic domain, much may be learned from a careful investigation of its classical counterpart.

However, in spite of the growing attention attracted by IFS, the explanation for this phenomenon is not yet completely clear, also, because theoretical analysis has to take into account a number of distinct dynamical features, the relative weight of which has not been fully assessed in determining IFS.

A typical example is the so-called "dichotomy." In a reference frame oscillating with the external field, the nucleus itself oscillates and produces an average Coulomb field quite similar to the field due to a charge continuously distributed along its trajectory. With a smooth (e.g., monochromatic) driving, the nucleus spends a large part of its time in the vicinity of the turning points of its trajectory; therefore, the effective charge distribution is highly nonhomogeneous and looks like a sort of dumbbell. At low field the combination of "dumbbell" and centrifugal potentials produces an effective potential well which has a single minimum; however, as the field increases the potential well is more and more strained, and above a certain field intensity it splits into a double-well potential which has two minima located close to the extrema of the dumbbell. This metamorphosis of the average potential experienced by the electron in the moving frame has attracted considerable attention, both in quantum [6] and in classical descriptions [3,5].

Generally speaking, the precise role of this and other intriguing features is not clear. Our understanding of the purely classical Kepler problem with a periodic driving is still far from complete, and further analysis is needed. For example, it is often argued, as an intuitive explanation of classical IFS, that the problem has *two* integrable limits, given respectively by the unperturbed Kepler motion and the free-field motion; the former limit is attained on neglecting the external field, the latter on neglecting interaction with the nucleus. On increasing the field intensity, the second limit is approached, and this should explain why the motion becomes stable.

This naive interpretation is not satisfactory, because the free-field motion is not bounded; it consists of oscillations *plus a drift* that would lead to fast ionization in an overwhelming majority of cases. As a matter of fact, at very large field intensities the survival probability drops to zero (see Fig. 1). In addition, the atomic part of the Hamiltonian is a *singular* perturbation of the free-field Hamiltonian: it is never "small" compared to the latter, because its effect is always quite strong in the proximity of the nucleus. Therefore, in order to explain IFS, one has to understand why, in the stabilized regime, the electron does not come close to the nucleus, even though it remains at all times confined in a bounded region.

In this paper we present results for a model of a classical 3D hydrogen atom subject to a periodic sequence of δ-like pulses of fixed strength and direction and alternating sign. The motion of the electron under such a driving is conveniently described in a stroboscopic way, by iterating a map that yields the evolution over one complete period of the external kicking field. In comparison with

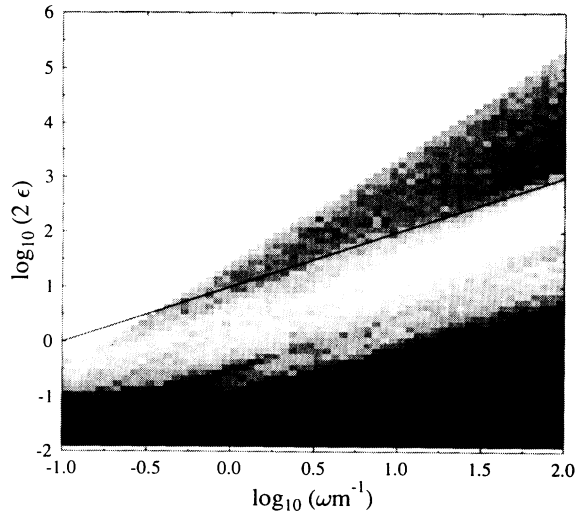

FIG. 1. Survival probability after a time ~ 1000 a.u. with microcanonically distributed initial conditions at $n=1$, $l=0.3$, and $m=0.25$, as a function of intensity ϵ and frequency ω, for 60 evenly spaced values on the horizontal axis and 80 evenly spaced values on the vertical axis. Darker tones of grey correspond to larger survival probability. The line has equation $\epsilon=5\omega/m$.

the monochromatically driven model, the kicked model offers the advantage of a much easier numerical simulation; at the same time, it turns out to retain many of the essential features of the monochromatic case, including IFS. Thus one can carry out extensive numerical computations to yield a fairly complete picture of the classical process leading to ionization.

In this paper we use numerical results for the kicked model as an illustration of the relative importance of the various mechanisms that have been considered in connection with IFS.

Our results confirm that classical IFS appears only with a nonzero value of the magnetic number (the component of angular momentum along the direction of polarization of the field) [3,2], and support the central role of a mechanism, qualitatively similar to the one described in Ref. [9], which was used in Ref. [2] to derive quantitative conditions for IFS. In fact, the conditions for field intensity and frequency under which IFS was observed in our model are fully consistent with these quantitative arguments. At the same time, a smooth switch-on of the field was *necessary* to observe IFS.

In addition, our results suggest a marginal role for dichotomy, because in the kicked model IFS is observed *in the absence* of dichotomy. In fact that free-field motion is here uniform, except for *sudden* inversions occurring at the turning points; therefore the effective charge density seen by the electron in the moving frame is uniform (a rod instead of a dumbbell) and the potential it produces has in all cases *a single* minimum.

The 3D kicked model has been also studied in a recent paper [7] in which similar conclusions are drawn about dichotomy. The authors of that paper were able to investigate the *quantum* dynamics of the model, which was found to exhibit stabilization. Unfortunately their results, which were obtained with a zero magnetic quantum number, do not allow for a quantitative comparison with the classical data presented below.

The usual model for IFS is described by the Hamiltonian

$$H(\mathbf{p},\mathbf{r},t)=\frac{p^2}{2}-\frac{1}{r}+\epsilon z\sin(\omega t)\ , \tag{1}$$

where $\mathbf{r}=(x,y,z)$ and atomic units are used. The radiation field is treated in the dipole approximation and is linearly polarized in the z direction. Here we shall instead consider the Hamiltonian

$$H(\mathbf{p},\mathbf{r},t)=\frac{p^2}{2}-\frac{1}{r}+\frac{2\epsilon z}{\omega}\sum_{-\infty}^{+\infty}(-1)^n\delta\left[t-n\frac{T}{2}\right]\ . \tag{2}$$

The evolution defined by (2) over one period $T=2\pi/\omega$ is given by a product of four maps. The first of these describes a free Keplerian motion over a time $T/2$, the second a "kick" which discontinuously changes p_z into $p_z+(2\epsilon/\omega)$; next comes one more free Kepler motion, followed by one more kick changing p_z by $-2\epsilon/\omega$. Iteration of this four-factor map yields a stroboscopic evolution defined by (2) which can be computed with considerably less numerical effort than that required for the simulation of (1) over a comparable number of periods.

A Kramers-Henneberger (KH) transformation can be performed to a reference frame which oscillates in the z direction according to a sawtooth,

$$z_0(t)=(-1)^n\left[\alpha-\frac{\epsilon}{\omega}\left[t-\frac{nT}{2}\right]\right]$$

$$\text{for } \frac{nT}{2}\le t\le\frac{(n+1)T}{2}\ .$$

Here $\alpha=\pi\epsilon/2\omega^2$ is the halfwidth of free-field oscillations. On canonically transforming (2) to the variables $\mathbf{p}',\mathbf{r}'$ of the moving frame, one obtains the KH Hamiltonian

$$H_{\mathrm{KH}}=\frac{p'^2}{2}-\frac{1}{|\mathbf{r}'-z_0(t)\mathbf{e}|}\ ,$$

where $\mathbf{e}$ is a unit vector in the field direction. One can expand the periodic potential appearing in H_{KH} in a Fourier series. The constant average term will be

$$V(\mathbf{r}')=-\frac{1}{T}\int_0^T\frac{dt}{|\mathbf{r}'-z_0(t)\mathbf{e}|}$$

$$=-\frac{1}{2\alpha}\ln\frac{\sqrt{\rho^2+(z'+\alpha)^2}+z'+\alpha}{\sqrt{\rho^2+(z'-\alpha)^2}+z'-\alpha}\ , \tag{3}$$

where $\rho=\sqrt{x^2+y^2}$. For $|z'|<\alpha$, the average potential has a logarithmic singularity at $\rho=0$. Introducing the momenta p_ρ, $p_{z'}$ the time-averaged KH Hamiltonian in cylindrical coordinates becomes

$$\overline{H_{\mathrm{KH}}}=\frac{p_\rho^2}{2}+\frac{p_{z'}^2}{2}+\frac{m^2}{2\rho^2}+V(\rho,z')\ . \tag{4}$$

Here m is the constant z component of the angular momentum. The average potential appearing in (4) is the

sum of (3) and the centrifugal potential. Therefore it has a single minimum at

$$z'=0\ ,\quad \rho=\frac{m^2}{\sqrt{2}}\left[1+\left[1+\frac{4\alpha^2}{m^4}\right]^{1/2}\right]^{1/2}\ . \tag{5}$$

In the case of a sinusoidal driving the effective potential still has a stationary point at $z'=0$, which, however, becomes a saddle point for $(\alpha/m^2)\geq 0.9$; then two distinct minima appear, and the potential becomes dichotomic. This is never the case with the present model. A picture of the averaged KH potential is shown in Fig. 2, for parameter values which correspond to stabilized motion, as discussed below.

On setting $z'=0$, $p_z'=0$ in (4), a reduced one-dimensional Hamiltonian is obtained, the orbits of which are also stable orbits for (4), and will be termed "radial orbits" in the following.

The dependence of the ionization probability on the field parameters ϵ and ω is illustrated by the "phase diagram" of Fig. 1, which displays the survival probability after a fixed physical time for different values of ϵ and ω. It was constructed in the following way. First we have chosen 60 evenly spaced points on the horizontal axis and 80 evenly spaced points on the vertical axis. Having thus discretized the region shown in Fig. 1 by means of 4800 points, for each of these we have numerically computed 100 orbits having initial action variables $n=1$, $l=0.3$, $m=0.25$, and randomly distributed angle variables. Due to well-known scaling properties, cases with initial $n\neq 1$ can be reduced to cases $n=1$ by using scaled variables ωn^3, ϵn^4, l/n, and m/n.

The survival probability was determined as the fraction of orbits that remained within a distance $r=500$ from the nucleus after a time corresponding to approximately 1000 Kepler periods at $n=1$. Kicks were smoothly switched on, i.e., ϵ was linearly increased from zero to its nominal value during a finite number of kicks (ten kicks for the case of Fig. 1).

The main qualitative feature of Fig. 1 is represented by two wedge-shaped regions of high survival probability. These regions are separated by a "death valley" that becomes deeper when moving to higher frequencies. The lower stable region is located at small ϵ and corresponds to a regime of dynamically stable motion; the upper region is the one corresponding to IFS.

Of course, the survival probability depends on time: during a longer interaction time, some of the surviving orbits contributing in the grey zones in Fig. 1 would ionize. At later times Fig. 1 would therefore overall turn to paler tones of grey, and its geography would be also modified. In Fig. 3 we show the dependence on time of the survival probability recorded at three different positions in the ϵ, ω plane of Fig. 1, namely, one deep in the lower stable region, another still in that region but not far from its upper border, and a third one inside the IFS region. In the first two cases the survival probability is not stable in time and will in fact decrease at larger times. Instead, in the third case the probability will at first decrease but then settle to a seemingly constant value.

Let us now discuss in more detail the various regions, starting with the lower stable one. According to Fig. 3, the upper border of this region is not constant in time and moves downwards on increasing the interaction time. This time-dependent border is determined by a chaotic ionization mechanism very similar to the one widely discussed for the case of monochromatic driving. This mechanism is qualitatively illustrated in Fig. 4, where we show an ionizing orbit very close to the border. Far from the nucleus the electron is moving on an almost perfect Keplerian ellipse in spite of the periodic kicks. In fact, subsequent kicks have opposite sign, and compensate for each other almost exactly, except when the electron comes close to the nucleus: there its velocity changes significantly between subsequent kicks, and the external

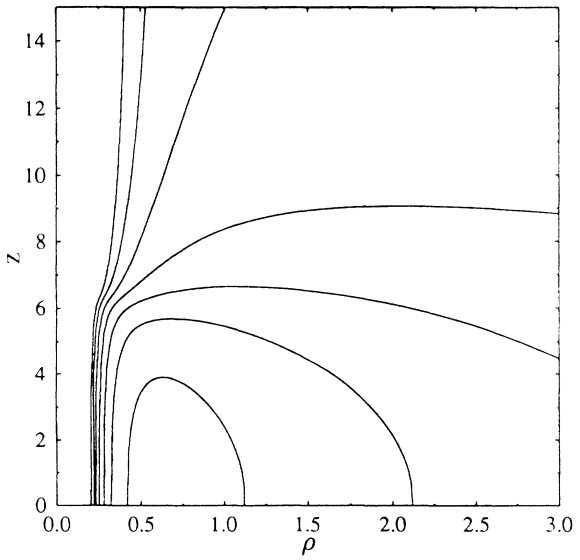

FIG. 2. Showing some equipotential lines of the average KH potential in the plane (ρ,z'), at $m=0.25$, $\epsilon=158$, and $\omega=6.28$. Since these lines are symmetric with respect to $z=0$, only the part lying in the region $z>0$ is shown.

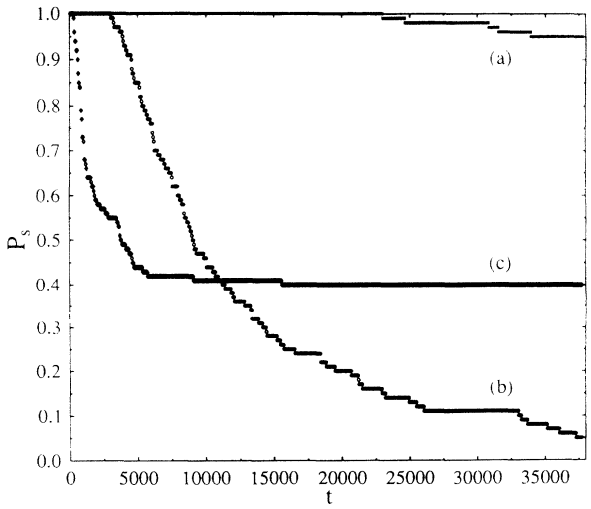

FIG. 3. Illustrating the dependence of the stabilization probability P_s on time, at fixed frequency $\omega=7.9$, for three different field intensities: (a) $\epsilon=0.2$, (b) $\epsilon=3.17$, and (c) $\epsilon=500$.

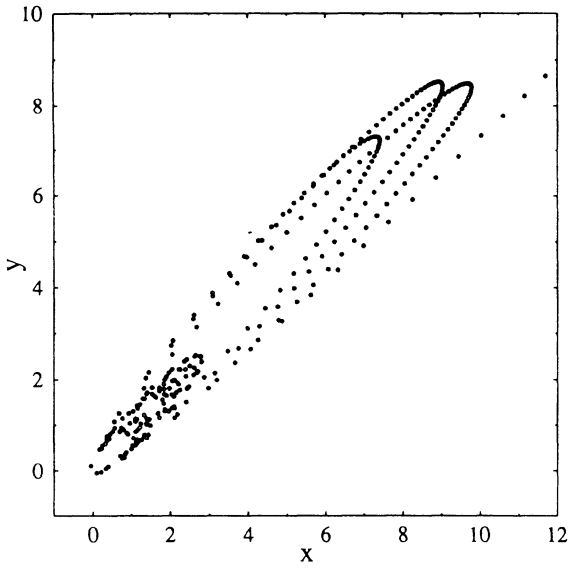

FIG. 4. An ionizing orbit with $n=1$, $m=0.25$, and initial value of $l=0.3$, projected onto the plane (x,y) of the initial unperturbed orbit, for $\epsilon=0.5$, and $\omega=6.28$.

field is therefore most effective. From close encounters with the nucleus the electron emerges on a different almost unperturbed ellipse and the process is repeated a number of times, until a particularly energetic encounter with the nucleus sets the electron on an escape route. In the case of monochromatic driving, the jumps from one unperturbed ellipse to another which occur when the electron comes close to the aphelion have been described by a "Kepler map," [8] which has a dynamically stable regime at small field intensities and becomes chaotic at strong fields. In the chaotic regime, the sequence of jumps can be pictured as a random walk (in energy) eventually leading to ionization. The corresponding diffusion coefficient, however, decreases on increasing the external frequency, so that at fixed interaction time the survival probability is found to be an increasing function of ω. The behavior observed in the kicked model is consistent with this general picture valid for the monochromatic case. Nevertheless, we ignore whether KAM tori exist at very small values of ϵ: these would leave Arnol'd diffusion as the only possible mechanism of long-time decay of the probability. Numerically computed Lyapunov exponents in the low-field regime fall in the range of numerical noise and are therefore consistent with either a KAM stability or a very weak level of chaoticity.

The time behavior shown by Fig. 3 suggests that the observed borders of the IFS region should not significantly change on increasing the interaction time. In Fig. 5 we give various representations of a typical stabilized orbit. The projection of this orbit on the plane of the initial unperturbed orbit fills an annulus-shaped region, which means in particular that the orbit never comes very close to the nucleus. The reason why such an orbit remains trapped apparently forever emerges when looking at its phase-space projection onto the (ρ,p_ρ) plane: after an initial transient this projection remains confined to a relatively narrow region, the shape of which is unambiguously tailored after the "radial orbits" of the averaged KH Hamiltonian. The width of this region is determined by the slow motion in the z direction. A numerical computation of the maximal Lyapunov exponent for orbits like the one shown in Fig. 5 yielded values $\sim 10^{-2}$, on the order of the numerical error; thus motion in the IFS region is either stable, or very weakly chaotic at best.

Another class of orbits exists in the IFS region, which account for the initial decay of the survival probability shown in Fig. 3(c). Once projected on the ρ,p_ρ plane, they are found to stick most of the time to some approximately periodic orbit whose period is very long compared to the period of the kicks; occasionally, and in coincidence with passages at minimal values of ρ, they jump from one such orbit to another, until eventually they escape. Again, the approximately periodic orbits mimicked by the projected dynamics are quite close to "radial" orbits.

It should be noted that, with monochromatic driving, the effect of coming close to the z axis is enhanced near the turning points of the nucleus, where the (dichotomic) potential has a worse singularity. In Ref. [7] it was pointed out that, due to this fact, the monochromatic case is less stable than the kicked one.

The above results substantiate the analysis of Ref. [2]. It assumes that, at sufficiently large ω, the average KH Hamiltonian will be an approximate constant of the motion [12]; the electron would then be trapped a long time inside the effective potential well, and the result of this trapping would be precisely IFS. Neglecting higher harmonics in the Fourier series is somewhat more problematic in the present case because their amplitude decays algebraically, and not exponentially as in the case of Hamiltonian (1); in any case, a rough estimate for the onset of IFS is obtained by requiring that the external frequency ω be larger than the internal frequency of oscillation in the potential well. Identifying the latter (in order of magnitude) with the frequency of small oscillations in the ρ direction around the minimum (5), we obtain the following estimate for the critical field strength at which IFS appears:

$$\epsilon_s \sim \text{const} \times \frac{\omega}{m} \ . \tag{6}$$

This estimate has the same functional dependence as for the sinusoidal driving. The essential point of this crude argument is that IFS is basically due to the low-frequency motion in the ρ direction being scarcely affected by high-frequency harmonics. This estimate is confirmed by our numerical results; indeed, the lower border of this IFS region in Fig. 1 appears to increase linearly with ω, as predicted by (6). Fitting this lower border yields a value ~ 5 for the constant in Eq. (6), to be compared with the value ~ 10 found for monochromatic driving [2]. The dependence on m is shown in Fig. 6, where the survival probability P_s is plotted versus m at fixed ω/m: P_s is roughly stationary as predicted by (6), but at small m a sharp fall is observed. Though not accounted for by the previous argument, this fall is explained by the growth of α as m is

decreased at fixed ratio ω/m: in fact, at very large α, the slow z motion will eventually carry the electron beyond the maximal distance $r \sim 500$ which defines ionization in our scheme.

The upper border of the IFS region in Fig. 1 clearly follows a ω^2 law. This can be understood on the following grounds. The potential well in the ρ direction is located around $\rho \sim m\epsilon^{1/2}/\omega$ and is therefore shifted to higher and higher values of ρ as the field is increased; it will eventually move so far that no orbit in the initial ensemble will have a chance to be trapped in it, because the initial ensemble of orbits has a finite extent in ρ that does not depend on ϵ and ω. The critical field for this effect will clearly scale as ω^2.

Finally, we have investigated the role of the switching-on process. In Fig. 7 we show the dependence of the survival probability on the field intensity at fixed frequency, for two different choices of the number of kicks during which the field is linearly increased to its nominal value. It is apparent that, with a sudden switch-on, IFS is practically suppressed. A smooth switch-on is therefore crucial in accommodating a consistent fraction of initial orbits inside the potential well, where they remain trapped. In this respect, IFS occurring in this model seems qualitatively similar to the "adiabatic" stabilization (see, e.g., Ref. [9]). However, a quantitative analysis of adiabaticity in a classical, periodically driven system in a chaotic regime is still an open problem [10].

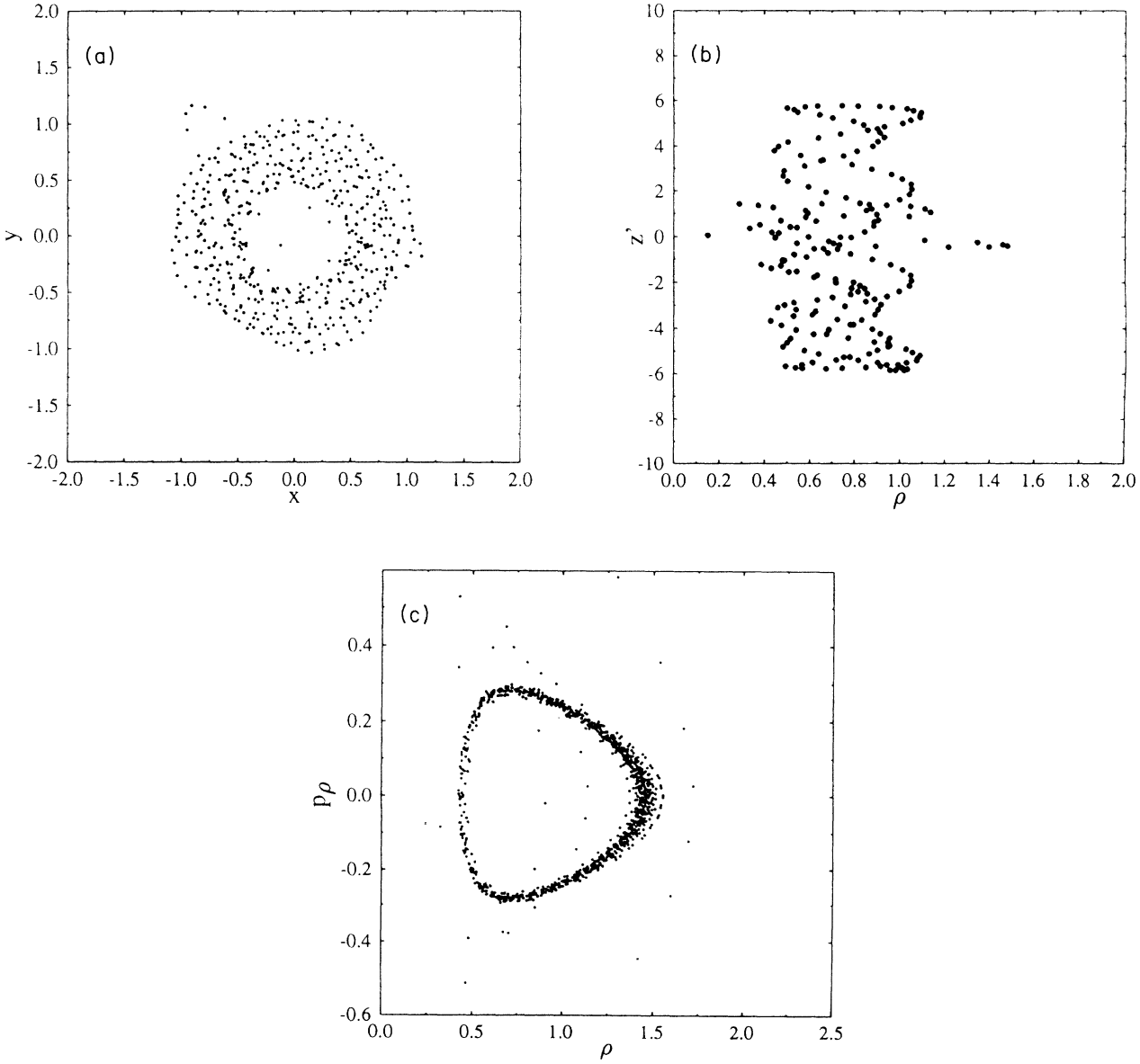

FIG. 5. A typical stabilized orbit at $n=1$, $m=0.25$, an initial value of $l=0.3$, $\epsilon=158$, and $\omega=6.28$, in different representations: (a) projection of the orbit-onto the plane (x,y) of the initial unperturbed orbit, (b) projection of the orbit onto the (ρ,z') plane in the moving frame, and (c) projection of the phase-space trajectory onto the (ρ,p_ρ) plane. Dotted lines in (c) represent orbits in the average KH potential at $z'=0$. The corresponding average KH potential is shown in Fig. 2.

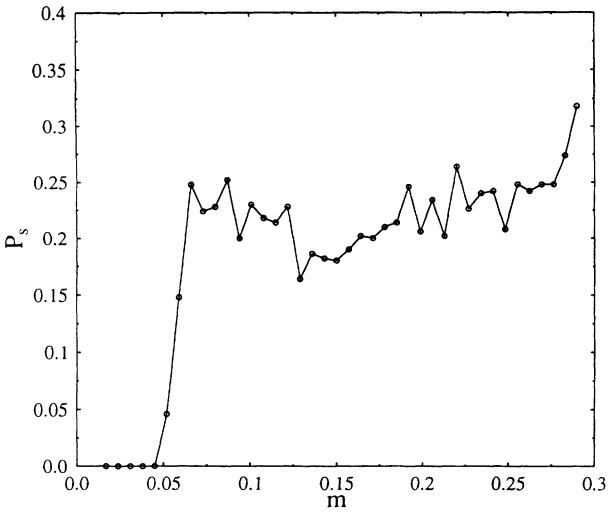

FIG. 6. Survival probability after a time $t=1000$ a.u. vs m at fixed ratio $\omega/m=1$ and fixed $\epsilon=0.629$, for a microcanonical ensemble of orbits with $n=1$ and $l=0.3$.

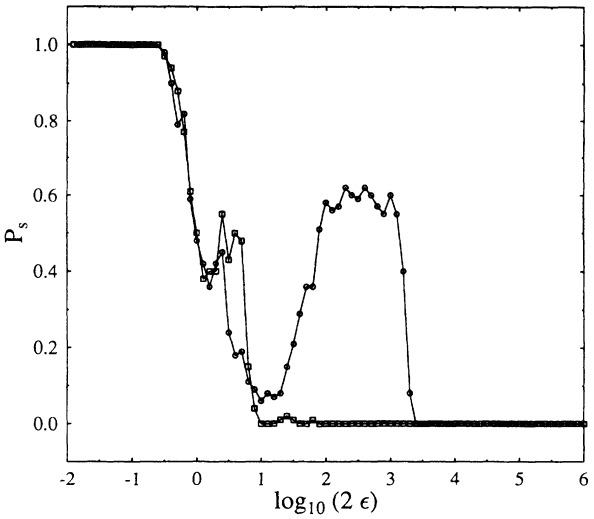

FIG. 7. Survival probability after a time $t=1000$ a.u. vs field intensity, at fixed $\omega=2.5$, for a microcanonical ensemble of orbits with $n=1$, $l=0.3$, $m=0.25$, and for two different values of the switch-on time t_s: circles are for $t_s=10$, squares for $t_s=1$.

In summary, we have investigated the IFS regime in a realistic model of a 3D hydrogen atom. In this model, classical IFS appears to be due to trapping of the radial motion (transverse to polarization of the field) inside the effective potential well. To a certain extent this trapping takes place independently of the structure of the potential well in the z direction; in particular, it does not rely on a bilocal, "dichotomic" structure of the latter, which is absent in this model. Our results quantitatively confirm the rough estimates previously given for the onset of IFS, and qualitatively substantiate the physical picture underlying them. In this picture IFS does not crucially depend on a large size of free-field oscillations, i.e., on the parameter α; in that case the stabilization border should scale with ω^2, and not with ω, as it was instead found.

Kicked dynamics, or maps, have been highly successful in the development of nonlinear dynamics, where they often retain in simplified form the essential features of more realistic continuous-time models. This was the main motivation of our investigation of the kicked Kepler dynamics, and appears to be fully justified by our results. The detailed scan of the parameter region presented in Fig. 1 was made possible by the map dynamics; producing a comparable picture with a monochromatic driving would require a significant computational effort.

In addition, we wish to add that, in contrast to the monochromatic case, periodic kicks involve all the harmonics of the basic kicking frequency. Therefore our results also have a bearing on the more general problem of the excitation of hydrogen atoms by multifrequency, "colored" driving, and related effects on IFS [11].

A final crucial question concerns the quantal relevance of the above classical results. On technical grounds, the quantized kicked model [7] does not appear to offer as many computational advantages with respect to a monochromatic model as the classical kicked model. In any case, under appropriate quasiclassical conditions the classical IFS should have a visible quantum counterpart. Such a quasiclassical IFS should not be expected to obey the purely quantum condition that the photon energy be larger than the electron binding energy; therefore, its investigation may substantially broaden the scope of current investigations of the intense-field stabilization effect.

[1] S. Geltman and M. R. Teague, J. Phys. B **7**, L22 (1974); J. I. Gersten and M. H. Mittleman, *ibid.* **9**, 2561 (1976); M. Gavrila and J. Z. Kaminsky, Phys. Rev. Lett. **52**, 614 (1984); M. V. Fedorov and A. M. Movsesian, J. Opt. Soc. Am. B **6**, 928 (1989); Q. Su, J. H. Eberly, and J. Javanainen, Phys. Rev. Lett. **64**, 862 (1990); M. Pont and M. Gavrila, *ibid.* **65**, 2362 (1990); K. C. Kulander, K. J. Schafer, and J. L. Krause, *ibid.* **66**, 2601 (1991); K. Burnett, P. L. Knight, B. R. M. Priraux, and V. C. Reed, *ibid.* **66**, 301 (1991); V. C. Reed, P. L. Knight, and K. Burnett, *ibid.*, **67**, 1415 (1991).

[2] F. Benvenuto, G. Casati, and D. L. Shepelyansky, Phys. Rev. A **47**, R786 (1993); Z. Phys. B **9** (1994).

[3] R. V. Jensen and B. Sundaram, Phys. Rev. A **47**, 1415 (1993); **47**, R778 (1993); Phys. Rev. Lett. **65**, 1964 (1992).

[4] Q. Su and J. H. Eberly, Phys. Rev. A **43**, 2474 (1991); R. Grobe and C. K. Law, *ibid.* **44**, 4114 (1991).

[5] J. Grochmalicki, M. Lewenstein, and K. Rzazewski, Phys. Rev. Lett. **66**, 1038 (1991).

[6] M. Pont, N. R. Walet, M. Gavrila, and C. W. McCurdy,

Phys. Rev. Lett. **61**, 939 (1988); J. H. Eberly, and K. C. Kulander, Science **262**, 1229 (1993).

[7] H. Wiedemann, J. Mostowski, F. Haake, Phys. Rev. A **49**, 1171 (1994).

[8] V. Gontis and B. Kaulakys, J. Phys. B **20**, 5051 (1987); G. Casati, I. Guarneri, and D. L. Shepelyansky, IEEE J. Quantum Electron. **24**, 1420 (1988).

[9] M. Pont and M. Gavrila, see Ref. [1]; Q. Su, J. H. Eberly, and M. Javanainen, see Ref. [1].

[10] J. P. Connerade, K. Conen, K. Dietz, and J. Henkel, Report No. BONN-AM-92-02, Bonn University (1992) (unpublished).

[11] C. M. Bowden, S. D. Pethel, C. C. Sung, and J. C. Englund, Phys. Rev. A **46**, 597 (1992); C. M. Bowden, C. C. Sung, S. D. Pethel, and A. B. Ritchie, *ibid.* **46**, 592 (1992).

[12] It is actually sufficient that $\omega n^3 > 1$.

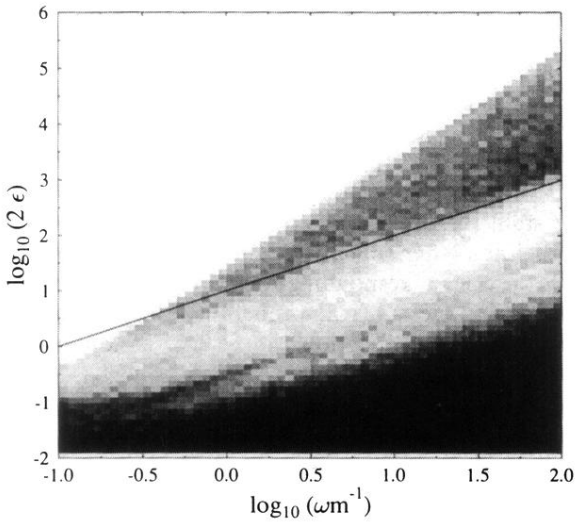

FIG. 1. Survival probability after a time ~ 1000 a.u. with microcanonically distributed initial conditions at $n=1$, $l=0.3$, and $m=0.25$, as a function of intensity ϵ and frequency ω, for 60 evenly spaced values on the horizontal axis and 80 evenly spaced values on the vertical axis. Darker tones of grey correspond to larger survival probability. The line has equation $\epsilon=5\omega/m$.